Title: Response Variability of Frontal Eye Field Neurons Modulates with Sensory Input and Saccade Preparation but not Visual Search Salience

Abbreviated Title: FEF response variability during search

Authors: Braden A. Purcell, Richard P. Heitz, Jeremiah Y. Cohen, Jeffrey D. Schall

Center for Integrative & Cognitive Neuroscience, Vanderbilt Vision Research Center, Department of Psychology, Vanderbilt University, Nashville, Tennessee 37240

Corresponding author:
Jeffrey D. Schall, Ph.D.
Department of Psychology
Vanderbilt University
PMB 407817
2301 Vanderbilt Place
Nashville, TN 37240-7817
jeffrey.d.schall@vanderbilt.edu
tel: (615) 322-0868
fax: (615) 343-5027

Pages: 52
Figures: 13
Tables: 1

Word count:
Abstract: 167
Introduction: 550
Discussion: 1730

Conflicts of interest: None

ABSTRACT

Discharge rate modulation of frontal eye field (FEF) neurons has been identified with a representation of visual search salience (physical conspicuity and behavioral relevance) and saccade preparation. We tested whether salience or saccade preparation are evident in the trial-to-trial variability of discharge rate. We quantified response variability via the Fano factor in FEF neurons recorded in monkeys performing efficient and inefficient visual search tasks. Response variability declined following stimulus presentation in most neurons, but despite clear discharge rate modulation, variability did not change with target salience. Instead, we found that response variability was modulated by stimulus luminance and the number of items in the visual field independent of attentional demands. Response variability declined to a minimum before saccade initiation and pre-saccadic response variability was directionally tuned. In addition, response variability was correlated with the response time of memory-guided saccades. These results indicate that the trial-by-trial response variability of FEF neurons reflects saccade preparation and the strength of sensory input, but not visual search salience or attentional allocation.

KEYWORDS: variability; Fano factor; attention; motor preparation; motor control

INTRODUCTION

Visually-responsive neurons in the frontal eye field (FEF) have been identified with a map of visual *salience* (Thompson and Bichot, 2005). By salience, we refer to the representation guiding the allocation of attention and gaze; some use the term *priority* (Bisley and Goldberg, 2010). The mean discharge rate of these neurons varies with the physical-conspicuity (bottom-up salience; Bichot and Schall, 1999a; Sato et al., 2001; Cohen et al., 2009) and behavioral relevance (top-down salience; Thompson et al., 1996; Bichot and Schall, 2002) of items in their response field (RF), regardless of whether a saccade is executed to the RF (Thompson et al., 1997; Thompson et al., 2005; Murthy et al., 2009). In addition, a distinct population of saccade-related neurons in FEF have been identified with saccade preparation (Bruce and Goldberg, 1985; Hanes and Schall, 1996; Boucher et al., 2007; Murthy et al., 2009; Purcell et al., 2010a; 2012a). The mean discharge rate of these neurons increases to a fixed threshold immediately prior to saccades (Hanes and Schall, 1996; Hanes et al., 1998). Thus far, the identification of FEF neurons with visual salience and saccade preparation is based entirely on changes in mean discharge rate.

Recent studies have demonstrated that the trial-by-trial variability of cortical neurons may be modulated by the behavioral relevance of objects in their RF. Response variability of V4 neurons declines with attention to an RF stimulus (Mitchell et al., 2007; Cohen and Maunsell, 2009). Reduced firing variability of neurons representing behaviorally relevant stimuli could improve the reliability with which a search target is discriminated and thereby improve search performance (Palmer et al., 2000). In FEF, neuronal response variability declines following stimulus onset, but is

not maintained in the absence of sensory input and the magnitude of the visually-evoked decline does not depend on whether or not the animal was cued to attend to the RF stimulus (Chang et al., 2012). A previous study from this laboratory reported that response variability of FEF neurons did not distinguish targets from distractors in distinct time intervals (Bichot et al., 2001), but the time course of response variability during visual search has never been systematically examined under differing attentional demands.

Other investigators have suggested that trial-by-trial variability can be a signature of motor preparation. Response variability in pre-motor cortex declines following presentation of a reach target and reaches a minimum immediately prior to arm movements (Churchland et al., 2006). Similar declines in variability prior to saccades have been reported in V4 (Steinmetz and Moore, 2010) and LIP (Churchland et al., 2011). The discharge rate dynamics of saccade-related FEF neurons can be explained by stochastic accumulator models that predict that response are initiated at a fixed threshold (Boucher et al., 2007; Purcell et al., 2010a; 2012a). If FEF neurons initiate saccades at a response threshold, as suggested by discharge rate modulation, then variability should be minimal at saccade initiation. It is not known whether the response variability of FEF neurons declines in a manner consistent with these models.

We computed the time-varying Fano factor as an index of response variability in FEF neurons recorded from monkeys performing a visual search task. If the response variability of FEF neurons depends on visual salience, then Fano factor should be modulated by the behavioral relevance and physical conspicuity of an RF stimulus. If response variability of FEF neurons depends on motor preparation, then Fano factor

should decline prior to saccade initiation. In addition, we would expect Fano factor to vary according to saccade direction and correlate with response time (RT).

METHODS

Behavioral tasks and recordings

We recorded single-unit spiking from the FEF of three macaques (*Macaca mulatta*). Monkeys were surgically implanted with a head post, a subconjunctive eye coil, and recording chambers during aseptic surgery under isoflurane anesthesia. Antibiotics and analgesics were administered postoperatively. All surgical and experimental procedures were in accordance with the National Institute of Health *Guide for the Care and Use of Laboratory Animals* and approved by the Vanderbilt Institutional Animal Care and Use Committee.

Neurons were recorded from both hemispheres of all monkeys using tungsten microelectrodes (2-4 MΩ, FHC) and were referenced to a guide tube in contact with the dura. All FEF recordings were acquired from the rostral bank of the arcuate sulcus at sites where saccades were evoked with low-intensity electrical microstimulation (<50 μA; Bruce et al., 1985). Spikes were sampled at 40 kHz. Waveforms were sorted online using a time-amplitude window discriminator and offline using principal component analysis and template matching (Plexon). Eye position was recorded at a sampling rate of 1kHz.

The monkeys performed visual search tasks of varying difficulty. Each monkey performed a subset of three variants of a search task in which either set size or target-

distractor similarity was manipulated. Basic analyses of these data have been published previously (Sato et al., 2001; Cohen et al., 2009; Purcell et al., 2010b).

In the first search task (Figure 1A), monkey F searched for a target (green or red disk) among seven distractors of the other color. Each trial began with the monkey fixating a central spot for ~600ms. A target was then presented at one of eight isoeccentric locations equally spaced around the fixation spot (8-10^{o} eccentricity). The other seven locations contained distractor stimuli. Search efficiency was varied randomly across trials by manipulating target-distractor similarity. For efficient search, distractors were red or green disks for green or red targets, respectively. For inefficient search, distractors were yellow-green disks for green targets. The monkey was rewarded for making a single saccade to the target and fixating it for ~400ms.

In the second search task (Figure 1B), monkeys Q and S searched for a target (T or L rotated 0^{o}, 90^{o}, 180^{o}, or 270^{o}) among distractors (rotated L or T). Each trial began with the monkey fixating a central spot for ~600ms. A target was then presented at one of eight isoeccentric locations equally spaced around the fixation spot (8-10^{o} eccentricity). The number of distractors varied randomly across trials (set size 2, 4, or 8). Stimuli were always arranged in diametrically opposite locations. The target and distractor identities remained constant throughout a session and target identity was varied across sessions. The monkey was rewarded for making a single saccade to the location of the target within 2000 ms of array onset and fixating the target for 500 ms.

In the third search task (Figure 1C), monkeys Q and S searched for a color target (green or red disks) among one, three, or seven distractors of the other color. The experimental protocol was otherwise identical to the form search. The form search task

was considered inefficient search and the color pop-out search task was considered efficient search based on behavioral patterns (see Results).

All monkeys performed a memory-guided saccade task to distinguish visual- from saccade-related activity (Hikosaka and Wurtz, 1983; Bruce and Goldberg, 1985). The target (filled gray circle) was presented without distractors for 80-150 ms. Monkeys were required to maintain fixation for 500-1000 ms after target onset. After the fixation point changed from filled to open, the monkeys were rewarded for making a saccade to the remembered location of the target and maintaining fixation for ~500ms. For monkeys Q and S, the target luminance was varied randomly across trials (0.01 to 8.05 cd/m^2). Unless otherwise stated, we used only trials in which target luminance was $\geq$0.99 cd/m^2 for basic analyses of this task because discharge rate and Fano factor varied little above this value.

Data analysis

For the search task, discharge rate and Fano factor were analyzed by sliding a 50 ms window in 10 ms steps across the spike train data. We verified that all visual search results were statistically indistinguishable using window sizes ranging from 10 to 150 ms. We used a larger window of 150 ms for the memory-guided saccade task because the average number of trials per condition (34 trials) was substantially less than search (110 trials). This provided additional smoothing at the expense of temporal smearing.

The discharge rate was calculated as the spike count in each time bin divided by the length of the window. The Fano factor was calculated as the ratio of the variance to

the mean of spike counts across trials within each time bin. Discharge rate and Fano factor were computed separately for each individual neuron, search condition, and stimulus in RF and then averaged across neurons. Trials with incorrect responses were excluded from neural analyses. Time bins in which the mean discharge rate was 0 were excluded from the average. Only well-isolated neurons in which the waveform and average discharge rates were stable across the recording session were included. Unless otherwise noted, all units were included for analysis regardless of whether task-related modulations were observed. Results were similar whether or not nonmodulated neurons were included.

The center of the RF was determined by vector summation of the normalized response to each target location during the memory-guided saccade task. The angle of the resultant vector gave the preferred response location. To be conservative, we considered locations within 45^{o} of the preferred angle to be inside the RF, which is slightly smaller than the average RF width at 10^{o} eccentricity (~51^{o}) (Purcell et al., 2012b). We verified that our results do not depend greatly on the exact size of the RF. Trials were sorted according to whether the target appeared inside the RF or diametrically opposite to the RF center. This ensured that at least one stimulus was present in the RF on every analyzed trial even when set size was <8.

Discharge rate and Fano factor modulations were assessed using identical statistical methods. To assess significant deviations from baseline, we compared discharge rate and Fano factor at each time bin to the average activity -100 to 0 ms relative to array onset (Wilcoxon rank-sum test, $p < 0.01$). The *visual latency* was defined as the time bin when activity first diverged from baseline and remained

significantly different for 5 consecutive time bins. Discharge rate and Fano factor in each bin were computed from spike counts in a window as described above. To assess target and saccade-direction selectivity, we compared the discharge rate and Fano factor when the target or distractors were inside the neurons' RFs (Wilcoxon rank-sum test, $p < 0.01$). The *selection time* was defined as the time bin when activity first significantly diverged and remained significantly different for 5 consecutive bins. We used a bootstrapping procedure to compute standard error and confidence intervals. We randomly sampled, with replacement, 1000 times from our population of neurons, computed the visual latency and selection time for each sample, and estimated the standard error and confidence intervals directly from the resulting distribution.

In addition to bin-by-bin statistical comparisons, we also analyzed discharge rate and Fano factor in three key epochs. For spike times relative to stimulus presentation, we defined the *post-stimulus* period as the time interval from 100 ms after array onset until 100 ms before mean saccade response time for each neuron. This epoch was computed separately for each neuron, but fixed across trials. We used this epoch to analyze the earliest period of visual selection that followed the initial non-selective visual response, but preceded saccade initiation. This epoch corresponds approximately to the earliest times at which the target location can first be discriminated in individual FEF neurons (e.g., Thompson et al., 1996; Cohen et al., 2009). Results were statistically indistinguishable using a more conservative window 100 to 150 ms relative to array onset for all neurons, which excluded saccades from all but ~1% of trials. For spike times relative to saccade, we defined the *pre-saccade* period as the time interval from 50 to 0 ms before saccade initiation. We used this epoch to analyze the state of motor

preparation immediately prior to saccade. This epoch allowed us to evaluate models of saccade preparation that predict reductions in variability before saccades of a particular direction (e.g., stochastic accumulator models). Results were statistically indistinguishable using a larger window of 100 to 0 ms before saccade initiation. During the memory-guided saccade task, we also analyzed the *pre-cue* interval -200 to 0 ms before cue (fixation point offset). We used this epoch to analyze spatial maintenance and motor preparation during the memory delay. Note that our selection of time epochs is not intended to imply serial processing of covert attention and saccade processing; rather, the two processes probably overlap temporally (Purcell et al., 2010a; 2012a).

To assess the effect of luminance on discharge rate and Fano factor, we divided responses according to target location and luminance for neurons recorded during the memory-guided saccade task. We grouped trials into three groups according to luminance (Low: 0.01 to 0.6 cd/m^2; Medium: 0.20 to 1.00 cd/m^2; High: 1.70 to 5.00 cd/m^2). These groupings were chosen such that the average number of trials per condition was sufficiently large and approximately equal across groups (~25 trials). We computed the slope of the least squares regression line for discharge rate and Fano factor in the post-target interval as a function of median luminance value for each group. It is likely that more complex nonlinear functions better explain the relationship between luminance and discharge rate or Fano factor (Albrecht and Hamilton, 1982), but we did not have sufficient data to more precisely quantify the relationship. Hence, our goal is only to show that discharge rate and Fano factor in FEF are monotonically modulated by stimulus luminance across the range of tested values. We used a 50 ms window

when computing the visual latency of mean discharge rates for improved temporal resolution.

To assess the effect of set size on discharge rate and Fano factor, we divided responses according to search condition and stimulus in receptive field. We averaged discharge rate and Fano factor across time bins for each set size in a running window (±20 ms, four time bins) incremented in time steps of 10ms. The window moved from array onset until 50 ms before mean saccade response time for set size 2 to avoid comparisons across set sizes before and after saccades had been initiated. At each time step, we computed the slope of the least squares regression line for discharge rate and Fano factor as a function of set size and assessed the statistical significance ($p < 0.01$). We also report the mean discharge rate and Fano factor in the window 50 to 125 ms following target onset because the strongest changes in response variability were observed in this early visual epoch.

We classified FEF neurons as visually-responsive or saccade-related based on responses during the memory-guided saccade task. We computed a visuomovement index (VMI) for each neuron as follows:

$$VMI = \frac{V-M}{V+M},$$

where V is the average discharge rate 50 to 200 ms following target onset and M is the average discharge rate 50 to 0 ms prior to saccade. The VMI is 1 for neurons with only visual responses and -1 for neurons with only saccade-related responses. To be classified as visually-responsive, the VMI must be greater than 0 and the discharge rate of a neuron must be significantly greater than baseline (-100 to 0 ms) following target onset (50 to 200 ms; Wilcoxon rank-sum test, $p < 0.01$). To be classified as saccade-

related, the VMI must be less than 0 and the discharge rate must be significantly greater than baseline immediately prior to saccade (-50 to 0 ms). We also analyzed the subset of pure visual neuron with significant modulation in the post-stimulus epoch, but no significant modulation in the pre-saccadic epoch. Neurons without significant modulation in either epoch were considered nonmodulated.

We quantified spatial tuning by dividing discharge rate and Fano factor by distance from RF center (in polar angle) and averaging across neurons and search conditions. RF center was defined as the stimulus location closest to the neuron's preferred response location. We fit the average discharge rate or Fano factor as a function of target location with a Gaussian function of the form:

$$A(\varphi) = B + R \times \exp\left(-{}^{1}\!/_{2}\left[\frac{\varphi-\Phi}{T_{\varphi}}\right]^{2}\right),$$

where activation (A) as a function of polar angle (φ) depends on the baseline (B), maximum/minimum response (R), optimum direction (Φ), and directional tuning (T_{φ}) (Bruce and Goldberg, 1985; Schall et al., 1995a). Tuning width was estimated by the standard deviation (T_{φ}) of the best fitting Gaussian curve. Previous reports have demonstrated that some neurons exhibit flanking suppression (Schall et al., 1995a; Schall et al., 2004), which is best explained by a Difference-of-Gaussian function, but we found that the simpler Gaussian function accounted for most of the variance in the epoch of interest (all $R^2 > 0.95$). The data were fitted with a Simplex routine (Nelder and Mead, 1965) implemented in MATLAB (fminsearch.m) to minimize the sum of squared deviations between observed and predicted values. Fitting was repeated 20-30 times with different initial points to prevent settling in local minima. We used nonparametric bootstrapping to compare estimated tuning width for discharge rates and

Fano factor (Efron and Tibshirani, 1993; Wichmann and Hill, 2001). We randomly sampled, with replacement, from the set of neurons and fit the Gaussian function to the data 500 times. Standard error and confidence intervals were determined from the resulting tuning width distribution.

We used a mean-matching procedure to control for a possible effect of discharge rate on Fano factor. This procedure has been described in detail elsewhere (Churchland et al., 2010). Briefly, the mean spike count was determined for each time bin, search condition, and stimulus in RF. The algorithm determined a common distribution of mean spike counts (but not variances) that can be found at all time points and for each stimulus-in-RF condition. We randomly eliminated mean counts from a given neuron and condition until a common distribution was achieved at each time point for both RF stimuli. The Fano factor was then computed at each time point using only the data points remaining in this common distribution. The process was repeated 10 times and averaged to control for variation due to random sampling. We independently mean-matched data aligned on target onset and saccade. We performed this analysis using the Variance Toolbox for MATLAB (Churchland et al., 2010; http://www.stanford.edu/~shenoy/GroupCodePacks.htm).

To assess the relationship between Fano factor and RT, we divided trials into short RT and long RT according to whether they were faster or slower than the median RT, respectively. This analysis was only performed on neurons recorded during the memory-guided saccade task because short RTs during visual search made it impossible to distinguish whether variation in Fano factor preceded the earliest eye movements. Trials were divided into RT groups individually for each neuron and target

location so these factors were not confounded across groups. We excluded the lower 10th and upper 90th percentiles to exclude unusually short and long RTs. RTs <100 ms were considered anticipatory and excluded from analysis.

Accumulator model simulations.

We implemented a simple accumulator model to compare with observed neurophysiology. The model was governed by the following differential equation:

$$dX = dt\left(-\frac{X}{\tau} + I(t)\right).$$

The model input, *I,* was set to baseline, *z*, until array onset plus some afferent delay, T_r, at which point it increased by an amount sampled from a Gaussian distribution with mean, *v*, and standard deviation *η*. RT was given as the time when activation, *X*, reached a fixed threshold, *a*, at which point *I* was reduced to baseline. The parameters, *z*, *v*, *η*, and *a*, were set to 0.2, 1.7, 0.1, and 155, respectively, to predict a distribution of RTs similar to that observed during our visual search tasks. All simulations began 500 ms prior to array onset to establish a stable baseline. We fixed T_r to 50 ms to account for afferent delays (Schmolesky et al., 1998; Pouget et al., 2005). The time constant, τ, was fixed at 100 ms. All simulations used an integration time step of *dt* = 1 ms.

We simulated 110 trials for 304 simulated neurons to match the statistical power of the experimental data. For each simulated neuron, we rescaled the parameters *z*, *v*, *η*, and *a* by a value sampled from a uniform distribution ranging from 0.8 to 1.2 to account for variability in average discharge rate across the population. For each simulated trial, we generated spike times according to a time-inhomogeneous Poisson process with mean rate given by the model dynamics for that simulation. Spike counts

were binned across time, and mean discharge rate and Fano factor were computed exactly as described above for experimental data.

RESULTS

Three monkeys performed variants of a visual search task requiring a single saccade to a target among distractors. Basic behavioral data have been described previously (Sato et al., 2001; Cohen et al., 2009; Purcell et al., 2010b). Monkey F performed a color search task in which search efficiency was varied randomly across trials by manipulating target-distractor similarity (Figure 1A). Mean RTs (±SE) were faster during efficient search (208 ± 16.8 ms) relative to inefficient search (251 ± 16.3 ms; $p < 0.001$; Wilcoxon signed-rank test). Percent correct was also higher during efficient (94 ± 1.2) relative to inefficient search (71 ± 1.2). Monkeys Q and S performed an inefficient form search task in which set size was varied across trials (Figure 1B). The search slope (RT by set size) was steep for both monkey Q (23 ± 1.6; $p < 0.001$; linear regression slope coefficient) and monkey S (11 ± 1.4; $p < 0.001$), confirming that the form search task is attentionally demanding. Monkeys Q and S also performed an efficient pop-out color search task in which set size was varied randomly across trials (Figure 1C). The search slope was shallow for both monkey Q (2 ± 0.8; $p < 0.01$) and monkey S (1 ± 1.0; $p = 0.51$), and significantly lower than form search for both monkeys (both $p < 0.001$; linear regression; set size and task interaction coefficient), confirming that attentional demands for the pop-out color search task are minimal. These behavioral patterns are consistent with well-established patterns of efficient and

inefficient search in humans (Duncan and Humphreys, 1989; Wolfe, 1998) and monkeys (Bichot and Schall, 1999b).

FEF response variability does not reflect behavioral relevance or physical conspicuity

We recorded activity from 304 FEF neurons while monkeys performed the visual search tasks. Of those, 133 neurons were recorded during singleton color search in which search efficiency varied randomly across trials (Monkey F; Figure 1A). Ninety-three neurons were recorded during an attentionally-demanding inefficient form search (59 from monkey Q, and 34 from monkey S; Figure 1B). Seventy-eight neurons were recorded during a pop-out color search (44 neurons from monkey Q, and 34 neurons from monkey S; Figure 1C). Our initial analyses use the full population of 304 neurons.

Figure 2 shows the average population discharge rate and Fano factor for trials in which a target or a distractor appeared in the RF of the neuron. The population discharge rate increases significantly above baseline following the onset of the array regardless of the behavioral relevance of the RF stimulus (Figure 2A). The latency of the response (±SE) was similar when a target (46 ± 7.7 ms) or distractor (47 ± 8.3 ms) was in the RF ($p > 0.05$, bootstrap, 1000 samples). Discharge rates are initially equivalent regardless of the stimulus in RF, but diverge over time to significantly discriminate the target location 127 ± 4.0 ms following array onset. This timing is consistent with estimates of selection time from individual neurons (Cohen et al., 2009). We quantified the magnitude of selectivity across the population by computing the difference in discharge rate when the target or distractors were in a neuron's RF during the post-stimulus epoch 100 to 150 ms (Figure 2C). The population fired significantly

greater on average when the target was in their receptive field (7 ± 0.6 sp/s; $p < 0.001$, Wilcoxon signed-rank test). This observation was consistent across search tasks and monkeys (Table 1). These results demonstrate the classic observation that the discharge rates of FEF neurons select the location of behaviorally relevant objects irrespective of stimulus features (see Schall and Thompson, 1999 for review).

Figure 2B shows the average Fano factor computed using the same neurons, conditions, and time bins. The average baseline Fano factor for the population of neurons is 1.2 ± 0.03, which indicates slightly less regular spiking than a Poisson model (Fano factor = 1.0), and is similar to values observed in visual cortex (Dean, 1981; Tolhurst et al., 1983; Softky and Koch, 1993). The population Fano factor declines following the onset of the array regardless of RF stimulus. The latency of the decline was similar for targets (56 ± 11.9 ms) and distractors (62 ± 9.5 ms; $p > 0.05$; bootstrap, 1000 samples), and was not significantly different from the visual latency of mean discharge rate (both $p > 0.05$). This is consistent with previously reported declines in the Fano factor of FEF neurons following stimulus onset (Chang et al., 2012), which is commonly found in cortical neurons (Churchland et al., 2010). In contrast to the modulations in mean discharge rate, the magnitude of the post-array decline in Fano factor was equivalent for targets and distractors. There is a weak and fleeting divergence around 180 ms that never attains statistical significance and can be attributed to variability in the timing of saccades. The average post-stimulus difference in Fano factor when the target or distractors were in the neuron's receptive field was not significantly different from 0 (Figure 2D; $p = 0.74$). This observation was consistent across nearly every individual data set (Table 1). Only the Fano factor of neurons

recorded from monkey F during inefficient search reached marginal significance, but the effect was opposite the expected direction (i.e., distractors were more reliably encoded than targets). Thus, response variability in FEF neurons declines following array onset, but does not distinguish behaviorally relevant targets from irrelevant distractors despite robust discharge rate modulation.

In addition to behavioral relevance, the discharge rate of FEF neurons varies with the physical conspicuity of objects in their receptive field (bottom-up salience; e.g., Bichot and Schall, 1999a). To test for an effect of physical conspicuity, we computed discharge rate and Fano factor separately for efficient and inefficient search. Only set size 8 trials were included to eliminate variability due to stimulus number. Figure 3 shows the discharge rate and Fano factor computed from efficient and inefficient search trials. As in previous reports, FEF discharge rates discriminate the location of the target significantly earlier during efficient search (112 ± 4.8 ms; Figure 3A) than inefficient search (150 ± 6.1 ms; $p < 0.01$; bootstrap, 1000 samples; Figure 3C) (Sato et al. 2001). In addition, the magnitude of discrimination was greater during inefficient search (10 ± 0.1 sp/s; $p < 0.001$; Wilcoxon rank-sum test).

Fano factor declined following array onset regardless of search efficiency, but it did not distinguish whether the target or a distractor was in the RF in either efficient or inefficient search (Figure 3B,D; Table 1). The average post-stimulus percent decline in Fano factor during efficient (-5.7 ± 1.69) and inefficient search (-8.1 ± 1.76) was statistically indistinguishable ($p = 0.20$). Although Figure 3 suggests a variation in baseline discharge rate and variability across tasks, this difference is driven primarily by across-neuron differences for the two data sets. For neurons that were recorded during

both efficient and inefficient search, we verified that no within-neuron baseline difference in search efficiency was observed in discharge rate (p = 0.36; Wilcoxon signed-rank) or Fano factor (p = 0.20). Thus, we see no evidence of changes in response variability with search efficiency, despite clear changes in mean discharge rate.

FEF response variability reflects the strength of sensory input.

The post-stimulus decline in Fano factor irrespective of behavioral relevance or physical conspicuity suggests that response variability is sensitive to sensory input independent of attentional allocation. To test this hypothesis, we measured Fano factor while varying the strength of sensory input using two manipulations. First, we systematically varied stimulus luminance during the memory-guided saccade task. The mean post-stimulus discharge rate increased with luminance (Figure 4A,C; 1.6 ± 0.13 sp/s/cd/m^2; p < 0.001; Wilcoxon signed-rank test). This effect was partially driven by a decrease in visual latency at high luminance levels (Low: 79 ± 7.3 ms; Medium: 74 ± 6.4 ms; High: 53 ± 5.1 ms), which is observed throughout the visual system including lateral geniculate nucleus (Maunsell et al., 1999), striate (Gawne et al., 1996) and extrastriate areas (Oram et al., 2002), and superior colliculus (White and Munoz, 2011). In addition, the magnitude of the post-stimulus Fano factor decline increased with luminance (Figure 4B,D; -0.1 ± 0.01 Fano factor/cd/m^2; p < 0.001). This effect was still apparent in the mean-matched Fano factor (Figure 4C, inset), indicating that the reduction cannot be solely attributed to increases in mean discharge rate. Neither discharge rate nor Fano factor showed significant modulation with luminance when the target appeared

outside the neuron's RF (both $p > 0.05$). Thus, increased sensory input decreases trial-by-trial response variability in FEF neurons.

Second, we manipulated the strength of sensory input by systematically varying the number of objects in the visual field. In the post-stimulus epoch, mean discharge rate significantly decreased as additional items appeared in the visual field (-0.914 ± 0.141 sp/s/item; $p < 0.001$; Cohen et al., 2009). In addition, Fano factor significantly decreased with additional items (-0.006 ± 0.003 per item; $p < 0.05$).

Interestingly, Fano factor modulation by set size was strongest shortly after stimulus onset, before an effect of set size on discharge rate was evident (Figure 5). Therefore, we also compared the effect of set size on discharge rate and Fano factor in this early visual epoch (50-125 ms). During the initial visual response, discharge rate did not vary with set size regardless of whether a target or distractor was in the neuron's RF (Figure 5A,B insets; both $p > 0.05$; Wilcoxon signed-rank test). Although the mean discharge rate was invariant across set size at this time, Fano factor still significantly declined with set size when both the target (-0.009 ± 0.0037 per item; $p < 0.05$) or distractors (-0.011 ± 0.0033 per item; $p < 0.001$) were inside the neuron's RF (Figure 5C,D insets). Thus, in search, more objects in the visual field leads to an early reduction of neuronal variability independent of later changes in discharge rate.

We next divided trials by search efficiency and combined across RF stimuli (Figure 6). If the decline in Fano factor with set size is due to increasing attentional demands, then it should be absent during efficient search. However, we found that Fano factor in the early visual epoch declined with set size for both inefficient (-0.012 ± 0.0050 per item; $p < 0.001$) and efficient (-0.007 ± 0.0021 per item; $p < 0.01$) search

(Figure 6B,D). There was no effect of set size on discharge rate at this time for either search task (Figure 6A,C; both $p > 0.05$; Wilcoxon signed-rank test). The decline in Fano factor with set size was slightly, but not significantly weaker during efficient search relative to inefficient search ($p = 0.19$). There are several reasons to believe that this is due to lower stimulus luminance and not decreased attentional demands. First, the variation of Fano factor with set size is present regardless of RF stimulus (Figure 5), and therefore lacks spatial specificity or sensitivity to object relevance. Second, the variation of Fano factor with set size appears ~50 ms after array onset, which corresponds to afferent delays in FEF (Schmolesky et al., 1998; Pouget et al., 2005), but is before attention-related signals are observed in discharge rate. Lastly, theories of visual attention predict that increased reliability should produce improved performance (Palmer et al., 2000), but FEF neurons fired more reliably as performance declined during inefficient search. Altogether, these results suggest that Fano factor in FEF is modulated by the strength of sensory input but not attentional demands.

FEF response variability reflects saccade preparation

In the preceding sections, we analyzed Fano factor in early time intervals aligned on stimulus presentation to determine how behavioral relevance, physical conspicuity, and the strength of sensory input influence response variability in FEF neurons. In addition to encoding visual salience, the discharge rates of FEF neurons have also been identified with saccade preparation (Hanes and Schall, 1996; Hanes et al., 1998; Murthy et al., 2009). Specifically, the mean discharge rates of saccade-related FEF neurons have been identified with accumulator models that predict saccades are

initiated when discharge rates reach a fixed threshold (Ratcliff et al., 2003; Boucher et al., 2007; Purcell et al., 2010a; 2012a). This implies that response variability should reach a minimum prior to saccades of a particular direction. We analyzed the Fano factor of FEF neurons relative to saccade initiation to determine whether changes in response variability were consistent with accumulator models of saccade preparation.

Figure 7 shows the population discharge rate and Fano factor aligned to the onset of saccades directed towards or away from the neuron's RF. The population discharge rate predicted the saccade direction 92 ± 5.2 ms before gaze shifted (Figure 7A). On average (±SE), neurons fired 21 ± 1.4 sp/s more when the saccade was directed towards versus away from the RF (Figure 7C; $p < 0.001$, Wilcoxon signed-rank test). The population Fano factor initially declined regardless of saccade direction, but evolved to predict saccade direction 58 ± 9.9 ms before the eyes moved (Figure 7B). Across the population, Fano factor was significantly lower when a saccade was made towards a neuron's RF (Figure 7D; -0.10 ± 0.01, $p > 0.05$). Importantly, the pre-saccadic magnitude of discrimination ($p = 0.95$) and percent Fano factor decline ($p = 0.53$) were statistically indistinguishable between efficient and inefficient search, which indicates that this pre-saccadic selectivity cannot be identified with visual salience. Although some individual data sets fail to reach statistical significance, this trend is consistent across all tasks and monkeys (Table 1). Thus, although FEF response variability was not affected by stimulus relevance, it robustly predicted the direction of an upcoming saccade.

A potential concern is that differences in pre-saccadic Fano factor could be confounded by differences in mean discharge rate. Higher discharge rates could

impose more regular spiking due to the spike refractory period (Kara et al., 2000; Mitchell et al., 2007). To control for this possibility, we recomputed Fano factor using a mean-matching procedure that subsamples neurons and conditions at each time point such that mean discharge rate remains constant across time and conditions (Churchland et al., 2010). In the post-stimulus epoch, the mean discharge rate is constant across time, but there is still a significant decline in the Fano factor regardless of stimulus relevance (Figure 8). There is a brief, late difference in Fano factor around 190 ms that can be attributed to saccade initiation. Most importantly, the pre-saccadic Fano factor is still significantly lower when saccades were made to the RF despite approximately identical discharge rates. Thus, changes in pre-saccadic Fano factor cannot be attributed to changes in mean discharge rate.

We quantified the resolution of pre-saccadic spatial tuning during visual search by fitting a Gaussian curve to the mean discharge rate and Fano factor as a function of distance from the RF center. Consistent with previous results, the mean discharge rates in the post-stimulus interval were well explained by a Gaussian function (R^2 = 0.99; Figure 9A; but see Schall et al., 1995a; Schall et al., 2004), but the Fano factor was constant across target locations (Figure 9B). In contrast, pre-saccadic mean discharge rates (Figure 9C; $R^2 > 0.99$) and Fano factor (Figure 9D; $R^2 = 0.96$) were both well explained by a Gaussian function. We used the standard deviation of the best fitting Gaussian curve as an index of tuning width. The pre-saccadic Fano factor tuning width ($65^o \pm 8.6^o$) was slightly, but significantly more broadly tuned than the mean discharge rate ($51^o \pm 2.4^o$; $p < 0.05$, nonparametric bootstrap, 500 samples). Thus, response variability in FEF neurons reaches a minimum only prior to saccades of a

particular direction. This is inconsistent with models of motor preparation that predict all neurons in a population reach a variability minimum irrespective of the movement (e.g., Churchland et al., 2006; Afshar et al., 2011).

Visually-responsive and saccade-related subpopulations

Previous studies have proposed that salience and saccade preparation are encoded by functionally distinct subpopulations of FEF neurons. Specifically, visually-responsive neurons are proposed to represent salience, whereas saccade-related neurons are thought to integrate salience to a response threshold (Purcell et al., 2010a; 2012a). We classified neurons as visually-responsive and saccade-related based on their responses during a memory-guided saccade task to test whether they showed distinct patterns of response variability during search. We classified 108 neurons as visually-responsive and 124 neurons as saccade-related. These analyses excluded 28 neurons that were nonmodulated and neurons that were not recorded during the memory-guided saccade task.

We first asked whether a representation of stimulus relevance is selectively present in visually-responsive neurons. Figure 10 shows the mean discharge rate and Fano factor as a function of time since the array onset. Discharge rates of both visually-responsive and saccade-related neurons evolve to select the target location at 154 ± 9.3 ms (Figure 10A, left) and 139 ± 5.5 ms (Figure 10C, left), respectively. The Fano factor significantly declined following array onset for both visually-responsive (Figure 10B, left) and saccade-related (Figure 10D, left) neurons, but Fano factor never significantly distinguished the RF stimulus in either population (both $p > 0.05$). This

indicates that response variability does not change with stimulus relevance in both subpopulations.

We next asked whether a representation of saccade preparation is selectively present in saccade-related neurons. Discharge rates of both visually-responsive and saccade-related neurons evolved to predict the saccade direction 58 ± 7.6 ms and 80 ± 9.1 ms before the eyes moved, respectively (Figure 10A, 10C, right). However, the temporal dynamics of Fano factor were distinctly different for the two populations. Visually-responsive neurons never significantly distinguished the saccade direction on a bin-by-bin basis (Figure 10B), whereas saccade-related neurons predicted the saccade direction 51.6 ± 11.6 ms before the eyes moved (Figure 10D; $p < 0.01$). Likewise, the subset of 43 pure visual neurons which showed significant post-stimulus modulation, but no significant pre-saccadic modulation also exhibited saccade-direction dependent modulation of discharge rate ($p < 0.001$), but not Fano factor ($p = 0.07$). The pre-saccadic Fano factor of visually-responsive neurons reached a minimum 75 ± 13.8 ms before saccade and increased before the eyes moved. Neurons in brainstem nuclei that control saccades become active ~15 ms prior to eye movements (Scudder et al., 2002), which means that variability has increased from the minimum when the saccade is triggered. In contrast, saccade-related neurons declined to a minimum immediately prior to saccades (3 ± 7.8 ms), which means that variability was nearing minimum when the saccade was triggered. There was also a significant positive correlation between VMI and pre-saccadic Fano factor ($r = 0.13$; $p < 0.05$), indicating that neurons with stronger saccade-related responses tended to have lower response variability prior to saccades. Altogether, the differences in pre-saccadic Fano factor suggest that saccade

preparation can be identified with saccade-related, but not visually-responsive neurons (see also Hanes et al., 1998; Brown et al., 2008).

Stochastic accumulator simulations

Saccade-related neurons have been identified with stochastic accumulators that initiate a saccade when discharge rates reach a fixed threshold (Ratcliff et al., 2003; Boucher et al., 2007; Purcell et al., 2010a; 2012a). However, many accumulator models predict that variability increases over time (Ratcliff, 1978; Churchland et al., 2011), which appears to be inconsistent with the post-stimulus decline in Fano factor (Figure 10D). We evaluated a simple stochastic accumulator model to test whether the basic predictions of this framework are consistent with the observed changes in response variability of FEF neurons. As expected, the model predicts a decline in Fano factor before saccade initiation because responses are initiated at a fixed discharge rate threshold (Figure 11, bottom right). Surprisingly, the model also predicts the decline in Fano factor following stimulus presentation (Figure 11, bottom left). Variability declines because the average increase in mean input following array onset (v-z) is greater than the increase in variability (η) that gives the model its variable rate of rise. As long as the ratio, $(v\text{-}z)/\eta$, is sufficiently high, the model will predict a post-stimulus decline in Fano factor. Critically, using the same parameterization, the model can predict an RT distribution comparable to the range observed during visual search tasks (Figure 11, top). We present this simple model as a proof of concept that the basic predictions of the accumulator model framework are consistent with response-variability dynamics observed in FEF. Systematic evaluation of alternative network architectures will be

necessary to fully explore potential mechanisms underlying saccade generation and their contribution to response variability.

Response variability during memory-guided saccades

It is possible that response variability does not change with visual search salience because response variability lacks spatial tuning. We analyzed response variability following the onset of a single target during the memory-guided saccade task to evaluate this possibility. Discharge rates increased when the target appeared inside the RF, but were unchanged when the target was outside the RF (Figure 12A). This produced significant selectivity following target onset (Figure 12C; 16 ± 1.2 sp/s; $p < 0.001$; Wilcoxon signed-rank test) that was maintained throughout the delay interval prior to the cue (9.8 ± 1.0 sp/s; $p < 0.001$) and the pre-saccadic epoch (14.9 ± 1.7 sp/s; $p < 0.001$). Thus, modulations in discharge rate were present throughout all critical task epochs.

In contrast, Fano factor declined when the target appeared inside or opposite the RF (Figure 12B). Importantly, the decline was greater when the target was inside the RF. This resulted in significant selectivity following target onset (-0.12 ± 0.04; $p < 0.001$; Wilcoxon signed-rank test), but Fano factor returned to baseline shortly after the target disappeared and selectivity was absent in the delay interval ($p > 0.05$). We verified that this effect was still present in the mean-matched Fano factor (Figure 12, insets), and therefore cannot be solely due to differences in mean discharge rate. This is consistent with a recent study showing that the post-stimulus response variability of FEF neurons is broadly tuned, but is not maintained in the absence of the stimulus even when the

location must later be used to guide saccades (Chang et al., 2012). In addition, we found that Fano factor declined prior to saccade initiation regardless of saccade direction. There was a tendency for variability to be lowest for saccades to the neuron's RF (Figure 12D), but this difference was not significant. This is probably due to increased end-point scatter in the absence of a visual target and reduced statistical power relative to the visual search data due to fewer recorded trials. Altogether, the pattern of Fano factor modulation during memory-guided saccades indicates that the absence of any influence of salience on response variability during search is not due to an absence of spatial selectivity in Fano factor and supports the hypothesis that strong modulation of Fano factor is more closely associated with sensory input and motor preparation.

Response variability and RT

Previous studies have found that response variability in extrastriate and premotor cortex correlates with RT (Churchland et al., 2006; Steinmetz and Moore, 2010). We analyzed Fano factor conditionalized on RT during memory-guided saccades in the epoch prior to the cue. Figure 13A shows the mean discharge rates aligned on cue. Prior to the cue, there was no significant difference in mean discharge rate across RT groups regardless of whether the saccade was made towards (p = 0.25; Wilcoxon signed-rank test) or away from the RF (p = 0.72). In contrast, Fano factor was lower in the pre-cue epoch when RT was faster regardless of whether the saccade was made towards (-0.05 ± 0.019; $p < 0.05$; Wilcoxon signed-rank) or away (-0.11 ± 0.072; $p < 0.05$) from the RF. When combining across saccade directions, this difference

remained significant for the subpopulation of saccade-related neurons (-0.05 ± 0.026; $p < 0.05$), but not visually-responsive neurons (-0.03 ± 0.033; $p = 0.47$), although a similar trend was evident. Pre-saccadic discharge rate and Fano factor did not depend on the speed of the response (Figure 13C-D; both $p > 0.05$), which is consistent with accumulator model predictions. These results support our conclusion that Fano factor reflects motor preparation in FEF and introduces new constraints on models of saccade generation.

DISCUSSION

We found that response variability of FEF neurons declines following stimulus presentation, but the magnitude of decline is equal for search targets and distractors. Response variability did not change with search efficiency, despite clear modulation of mean discharge rate. Instead, we found that response variability was modulated by the strength of sensory input and declined to minimum before saccades to a neuron's RF. These results inform models of visual search and saccade generation.

Relation to theories of visual search and attention

Theories of visual search propose that a salience map guides attention and eye movements to locations of maximal activation (Itti and Koch, 2001; Bundesen et al., 2005; Wolfe, 2007). FEF is part of a network of oculomotor areas including superior colliculus and lateral intraparietal area, but not supplementary eye field (Purcell et al. 2012b), that have been identified with the salience map (Findlay and Walker, 1999; Thompson and Bichot, 2005; Gottlieb, 2007; Bisley and Goldberg, 2010). According to

this framework, the decline in response variability that we observed following stimulus presentation could improve the reliability with which the location of maximal activation can be distinguished. Importantly, declines in variability irrespective of stimulus salience, as we observed, will still improve target discriminability. In other words, target discriminability is increased by a reduction in variability for both the noise (distractor) and noise + signal (target) distributions. Thus, our observation that variability declines equally irrespective of object relevance could improve detection of the point of maximal activation throughout the neurophysiological salience map. These results are consistent with a previous study that failed to find target-distractor differences in FEF variability during search (Bichot et al., 2001), but that study only analyzed stimulus-aligned responses during the initial nonselective visual response (0 to 50 ms). Here, we show that response variability in FEF is not modulated by stimulus salience (relevance or conspicuity) during visual search during epochs in which large modulations in mean discharge rate are observed. This observation is also consistent with a previous study which found that the mean discharge rate, but not response variability, of FEF neurons was modulated when animals were cued to attend to the neuron's RF (Chang et al., 2012). Our results extend this observation to visual search tasks in which the target must be discriminated from among distractors to appropriately allocate attention (i.e., exogenous attention).

Considered in a signal detection theory framework, changes in behavioral performance with search efficiency could potentially be explained by increases in response magnitude (target enhancement) or decreases in response variability (noise reduction). We found that the discharge rates, but not response variability, of FEF

neurons was modulated by search efficiency, which supports a target enhancement model of attentional selectivity in FEF (Chang et al., 2012). This contrasts with observations in V4, in which spatial attention reduces response variability (Mitchell et al., 2007; Cohen and Maunsell, 2009). Similarly, although attention has been found to reduce trial-by-trial discharge rate correlations in V4 (Cohen and Maunsell, 2009; Mitchell et al., 2009) and MT (Cohen and Newsome, 2008), FEF neurons show increased correlations when search targets fall within the overlapping RFs of two neurons (Cohen et al., 2010). Thus, although both V4 and FEF neurons show modulation of discharge rate with behavioral relevance (e.g., Zhou and Desimone, 2011) and FEF is proposed to be a source of attentional modulations in V4 (Moore and Armstrong, 2003; Gregoriou et al., 2012), measures of response variability and correlated rate variations suggest very different mechanisms of selection are operating in frontal and posterior visual areas.

This result also challenges models of attention which propose a serial scan of locations on the salience map (e.g., Treisman and Gelade, 1980; see also Buschman and Miller, 2009). Serial search, which entails greater variability in the time when attention is focused on an object, should produce greater variability in discharge rate during inefficient search. Our observation that Fano factor declines equivalently for efficient and inefficient search is inconsistent with this implication.

Stronger sensory input decreases response variability

Discharge rate increases with luminance-contrast throughout the visual system (Dean, 1981; Albrecht and Hamilton, 1982; Schiller and Colby, 1983; Tolhurst et al.,

1983). This includes neurons in extrastriate areas V4 and superior temporal sulcus (Reynolds et al., 2000; Oram et al., 2002) that project topographically to FEF (Huerta et al., 1987; Stanton et al., 1988; Schall et al., 1995b). Thus, increasing luminance can be identified with increasing the strength of sensory input to FEF. We found that FEF neurons fired more consistently following the onset of higher luminance stimuli. Similar declines in variability are observed in LGN neurons with increased retinal stimulation and microstimulation of afferent sources (Hartveit and Heggelund, 1994). Moreover, the effect was preserved after mean-matching, which indicates that the improvement must be due to decreases in noise above and beyond increases in mean discharge rates. This indicates an improved signal-to-noise ratio for higher luminance stimuli that could be partially responsible for variations in performance during visually-guided saccades to targets of varying luminance (Carpenter, 2004).

During memory-guided saccades, response variability declined following presentation of a single target anywhere in the visual field, but the decline was greatest in the neuron's RF. This is consistent with a recent study, which found broad tuning of response variability in FEF in response to single targets (Chang et al., 2012). The monkeys in the Chang et al. (2012) study were trained to remember the target location in order to perform a subsequent change detection task. Unlike that study, our monkeys were trained to make a saccade to the location of the remember target, and therefore could begin preparing a saccade to the remembered location during the delay interval. We observed an additional decline in Fano factor as the time of saccade approaches that was similar to the decline observed in neurons recorded from the dorsolateral pre-frontal cortex of macaques performing a visual discrimination task

(Hussar and Pasternak, 2010). Like Chang et al. (2012), we found that selectivity vanishes shortly after the stimulus is removed despite sustained discharge rates during the memory delay. This provides converging evidence that maintenance of spatial information in the absence of sensory input does not alter response variability. Unlike sensory input, which is necessarily feed-forward, maintenance of spatial information is thought to be implemented through local recurrent excitation (Wang, 1999; Compte et al., 2000). Therefore, our results are consistent with the hypothesis that feed-forward, but not recurrent, excitation causes a decline in response variability. This hypothesis is also supported by the observation that inactivation of primary visual cortex via electrical stimulation does not alter variability in membrane potential, and changes in variability with contrast can be entirely accounted for by changes in variability in feedforward inputs form the lateral geniculate nucleus (Sadagopan & Ferster, 2012).

Response variability modulates with saccade preparation

During the visual search task, response variability declined to a minimum before saccades. This result was unexpected because a previous study failed to find differences in pre-saccadic response variability (Bichot et al., 2001). This is probably because Bichot et al. (2001) included mostly visually-responsive neurons, which were found to show little to no pre-saccadic Fano factor selectivity. Importantly, we found that variability was minimal only for saccades directed to the neuron's RF. The population Fano factor was only slightly more broadly tuned than discharge rates prior to saccade initiation, which is consistent with observations that pre-saccadic response variability reaches a minimum before saccades to the RF in LIP (Churchland et al.,

2011). In contrast, response variability in pre-motor cortex was found to be invariant across arm reaches in different directions (Churchland et al., 2006) and the influence of saccade direction on Fano factor variability in V4 is weak (Steinmetz and Moore, 2010). Weak spatial tuning of response variability has been interpreted in support of an 'optimal subspace hypothesis' in which all neurons in a cortical area initiate a movement when discharge rates converge to a specific value (Afshar et al., 2011). The observation that pre-saccadic Fano factor is sharply tuned in FEF neurons means that only neurons that encode the end-point of the upcoming saccade are reaching a minimum variance. Moreover, we showed that only saccade-related, but not visually-responsive, neurons reach a minimum variance before saccades. Altogether, these results suggest that the optimal subspace hypothesis does not generalize to the oculomotor system.

Saccade-related FEF and SC neurons have been identified with stochastic accumulators to a response threshold that is invariant with RT within a condition (Ratcliff et al., 2003; Boucher et al., 2007; Purcell et al., 2010a; 2012a). The most basic prediction of this framework is that variability should decline to a minimum at the time of the response. We showed that saccade-related neurons conform to this prediction. Many forms of stochastic accumulator models also predict an increase in variability as a function of time (e.g., Ratcliff, 1978; Carpenter and Williams, 1995; Brown and Heathcote, 2005), which is inconsistent with the post-stimulus decline in response variability that we observed. However, we demonstrated that a simple accumulator model can predict both the decline in response variability and RT distributions corresponding to those observed during visual search. The model demonstrates that

Fano factor will decline so long as the increase in mean input following array onset is sufficiently larger than the increase in variability that produces varying rates of rise. Future modeling work will be necessary to rule out network architectures that fail to predict this decline in variability.

During memory-guided saccades, RTs were fastest when variability was lower prior to the imperative stimulus. This is consistent with our conclusion that response variability in FEF reflects saccade preparation. Similar correlations between response variability and RT have been observed in premotor cortex (Churchland et al., 2006) and V4 (Steinmetz and Moore, 2010). In premotor cortex, this observation has been interpreted as evidence that pools of neurons are approaching an optimal discharge rate (Afshar et al., 2011; Churchland et al., 2006), but our results indicate that, at least for the oculomotor system, accumulator models provide a complete account of saccade preparation and initiation. Why then does variability decline before fast saccades? Several potential mechanisms can cause reduce variability without influencing discharge rates, for example increases in balanced excitation and inhibition or self-inhibition. Thus, this result provides additional constraint on computational models of saccade choice and decision-making.

ACKNOWLEDGEMENTS

We thank D. Godlove and P. Weigand for useful discussion throughout the preparation of this work. JYC current address is Department of Molecular and Cellular Biology, Center for Brain Science, Harvard University, Cambridge, Massachusetts 02138, USA

GRANTS

This work was supported by National Institutes of Health Grants T32EY07135, R01EY08890, P30EY008126, P30HD015052, and Robin and Richard Patton through the E. Bronson Ingram Chair in Neuroscience.

AUTHOR CONTRIBUTIONS

BAP and JDS designed research; BAP, RPH, and JYC performed research; BAP analyzed data; BAP and JDS wrote the paper

REFERENCES

Afshar A, Santhanam G, Yu BM, Ryu SI, Sahani M, and Shenoy KV. Single-trial neural correlates of arm movement preparation. *Neuron* 71: 555-564, 2011.

Albrecht DG, and Hamilton DB. Striate cortex of monkey and cat: Contrast response function. *J Neurophysiol* 1982.

Bichot NP, and Schall JD. Effects of similarity and history on neural mechanisms of visual selection. *Nat Neurosci* 2: 549-554, 1999a.

Bichot NP, and Schall JD. Priming in macaque frontal cortex during popout visual search: feature-based facilitation and location-based inhibition of return. *J Neurosci* 22: 4675, 2002.

Bichot NP, and Schall JD. Saccade target selection in macaque during feature and conjunction visual search. *Visual Neurosci* 16: 81-89, 1999b.

Bichot NP, Thompson KG, Rao SC, and Schall JD. Reliability of macaque frontal eye field neurons signaling saccade targets during visual search. *J Neurosci* 21: 713-725, 2001.

Bisley JW, and Goldberg ME. Attention, intention, and priority in the parietal lobe. *Annu Rev Neurosci* 33: 1-21, 2010.

Boucher L, Palmeri TJ, Logan GD, and Schall JD. Inhibitory control in mind and brain: An interactive race model of countermanding saccades. *Psychol Rev* 114: 376, 2007.

Brown JW, Hanes DP, Schall JD, and Stuphorn V. Relation of frontal eye field activity to saccade initiation during a countermanding task. Exp Brain Res 190: 135-151, 2008.

Brown S, and Heathcote A. A ballistic model of choice response time. *Psychol Rev* 112: 117-128, 2005.

Bruce CJ, and Goldberg ME. Primate frontal eye fields. I. Single neurons discharging before saccades. *J Neurophysiol* 53: 603-635, 1985.

Bruce CJ, Goldberg ME, Bushnell MC, and Stanton GB. Primate frontal eye fields. II. Physiological and anatomical correlates of electrically evoked eye movements. *J Neurophysiol* 54: 714, 1985.

Bundesen C, Habekost T, and Kyllingsbæk S. A neural theory of visual attention: Bridging cognition and neurophysiology. *Psychol Rev* 112: 291-328, 2005.

Buschman TJ, and Miller EK. Serial, covert shifts of attention during visual search are reflected by the frontal eye fields and correlated with population oscillations. *Neuron* 63: 386-396, 2009.

Carpenter RHS. Contrast, probability, and saccadic latency: Evidence for independence of detection and decision. *Curr Biol* 14: 1576-1580, 2004.

Carpenter RHS, and Williams MLL. Neural computation of log likelihood in control of saccadic eye movements. *Nature* 377: 59-62, 1995.

Chang MH, Armstrong KM, and Moore T. Dissociation of Response Variability from Firing Rate Effects in Frontal Eye Field Neurons during Visual Stimulation, Working Memory, and Attention. *J Neurosci* 32: 2204-2216, 2012.

Churchland AK, Kiani R, Chaudhuri R, Wang XJ, Pouget A, and Shadlen MN. Variance as a signature of neural computations during decision making. *Neuron* 69: 818-831, 2011.

Churchland MM, Byron MY, Cunningham JP, Sugrue LP, Cohen MR, Corrado GS, Newsome WT, Clark AM, Hosseini P, and Scott BB. Stimulus onset quenches neural variability: a widespread cortical phenomenon. *Nat Neurosci* 13: 369-378, 2010.

Churchland MM, Byron MY, Ryu SI, Santhanam G, and Shenoy KV. Neural variability in premotor cortex provides a signature of motor preparation. *J Neurosci* 26: 3697-3712, 2006.

Cohen JY, Crowder EA, Heitz RP, Subraveti CR, Thompson KG, Woodman GF, and Schall JD. Cooperation and competition among frontal eye field neurons during visual target selection. *J Neurosci* 30: 3227-3238, 2010.

Cohen JY, Heitz RP, Woodman GF, and Schall JD. Neural basis of the set-size effect in frontal eye field: timing of attention during visual search. *J Neurophysiol* 101: 1699-1704, 2009.

Cohen MR, and Maunsell JHR. Attention improves performance primarily by reducing interneuronal correlations. *Nat Neurosci* 12: 1594-1600, 2009.

Cohen MR, and Newsome WT. Context-dependent changes in functional circuitry in visual area MT. *Neuron* 60: 162-173, 2008.

Compte A, Brunel N, Goldman-Rakic PS, and Wang XJ. Synaptic mechanisms and network dynamics underlying spatial working memory in a cortical network model. *Cereb Cortex* 10: 910-923, 2000.

Dean AF. The variability of discharge of simple cells in the cat striate cortex. *Exp Brain Res* 44: 437-440, 1981.

Duncan J, and Humphreys GW. Visual search and stimulus similarity. *Psychol Rev* 96: 433, 1989.

Efron B, and Tibshirani R. *An introduction to the bootstrap*. Chapman & Hall/CRC, 1993.

Findlay JM, and Walker R. A model of saccade generation based on parallel processing and competitive inhibition. *Behav Brain Sci* 22: 661-674, 1999.

Gawne TJ, Kjaer TW, and Richmond BJ. Latency: another potential code for feature binding in striate cortex. *J Neurophysiol* 76: 1356-1360, 1996.

Gottlieb J. From thought to action: the parietal cortex as a bridge between perception, action, and cognition. *Neuron* 53: 9-16, 2007.

Gregoriou GG, Gotts SJ, and Desimone R. Cell-Type-Specific Synchronization of Neural Activity in FEF with V4 during Attention. *Neuron* 73: 581-594, 2012.

Hanes DP, Patterson WF, and Schall JD. Role of frontal eye fields in countermanding saccades: visual, movement, and fixation activity. *J Neurophysiol* 79: 817-834, 1998.

Hanes DP, and Schall JD. Neural control of voluntary movement initiation. *Science* 274: 427-430, 1996.

Hartveit E, and Heggelund P. Response variability of single cells in the dorsal lateral geniculate nucleus of the cat. Comparison with retinal input and effect of brain stem stimulation. *J Neurophysiol* 72: 1278-1289, 1994.

Hikosaka O, and Wurtz RH. Visual and oculomotor functions of monkey substantia nigra pars reticulata. IV. Relation of substantia nigra to superior colliculus. *J Neurophysiol* 49: 1285-1301, 1983.

Huerta MF, Krubitzer LA, and Kaas JH. Frontal eye field as defined by intracortical microstimulation in squirrel monkeys, owl monkeys, and macaque monkeys II. Cortical connections. *J Comp Neurol* 265: 332-361, 1987.

Hussar C, and Pasternak T. Trial-to-trial variability of the prefrontal neurons reveals the nature of their engagement in a motion discrimination task. *P Natl Acad Sci* 107: 21842-21847, 2010.

Ipata AE, Gee AL, Goldberg ME, and Bisley JW. Activity in the lateral intraparietal area predicts the goal and latency of saccades in a free-viewing visual search task. *J Neurosci* 26: 3656-3661, 2006.

Itti L, and Koch C. Computational modelling of visual attention. *Nat Rev Neurosci* 2: 194-203, 2001.

Kara P, Reinagel P, and Reid RC. Low response variability in simultaneously recorded retinal, thalamic, and cortical neurons. *Neuron* 27: 635-646, 2000.

Maunsell JHR, Ghose GM, Assad JA, McAdams CJ, Boudreau CE, and Noerager BD. Visual response latencies of magnocellular and parvocellular LGN neurons in macaque monkeys. *Visual Neurosci* 16: 1-14, 1999.

Mitchell JF, Sundberg KA, and Reynolds JH. Differential attention-dependent response modulation across cell classes in macaque visual area V4. *Neuron* 55: 131-141, 2007.

Mitchell JF, Sundberg KA, and Reynolds JH. Spatial attention decorrelates intrinsic activity fluctuations in macaque area V4. *Neuron* 63: 879-888, 2009.

Moore T, and Armstrong KM. Selective gating of visual signals by microstimulation of frontal cortex. *Nature* 421: 370-373, 2003.

Murthy A, Ray S, Shorter SM, Schall JD, and Thompson KG. Neural control of visual search by frontal eye field: effects of unexpected target displacement on visual selection and saccade preparation. *J Neurophysiol* 101: 2485-2506, 2009.

Nelder JA, and Mead R. A simplex method for function minimization. *The computer journal* 7: 308, 1965.

Oram MW, Xiao D, Dritschel B, and Payne KR. The temporal resolution of neural codes: does response latency have a unique role? *Philosophical Transactions of the Royal Society of London Series B: Biological Sciences* 357: 987-1001, 2002.

Palmer J, Verghese P, and Pavel M. The psychophysics of visual search. *Vision Res* 40: 1227-1268, 2000.

Pouget P, Emeric EE, Stuphorn V, Reis K, and Schall JD. Chronometry of visual responses in frontal eye field, supplementary eye field, and anterior cingulate cortex. *J Neurophysiol* 94: 2086, 2005.

Purcell BA, Heitz RP, Cohen JY, Schall JD, Logan GD, and Palmeri TJ. Neurally constrained modeling of perceptual decision making. *Psychol Rev* 117: 1113-1143, 2010a.

Purcell BA, Schall JD, Logan GD, and Palmeri TJ. From Salience to Saccades: Multiple-Alternative Gated Stochastic Accumulator Model of Visual Search. *J Neurosci* 32: 3433-3446, 2012a.

Purcell BA, Heitz RP, Cohen JY, Woodman GF, and Schall JD. Timing of attentional selection in frontal eye field and event-related potentials over visual cortex during pop-out search. *J Vis* 10: 2010b.

Purcell BA, Weigand PK, and Schall JD. Supplementary Eye Field during Visual Search: Salience, Cognitive Control, and Performance Monitoring. J Neurosci 32: 10273-10285, 2012b.

Ratcliff R. A theory of memory retrieval. *Psychol Rev* 85: 59, 1978.

Ratcliff R, Cherian A, and Segraves M. A comparison of macaque behavior and superior colliculus neuronal activity to predictions from models of two-choice decisions. *J Neurophysiol* 90: 1392-1407, 2003.

Reynolds JH, Pasternak T, and Desimone R. Attention increases sensitivity of V4 neurons. *Neuron* 26: 703-714, 2000.

Sadagopan S, and Ferster D. Feedforward Origins of Response Variability Underlying Contrast Invariant Orientation Tuning in Cat Visual Cortex. Neuron 74: 911-923.

Sato T, Murthy A, Thompson KG, and Schall JD. Search efficiency but not response interference affects visual selection in frontal eye field. *Neuron* 30: 583-591, 2001.

Schall JD, Hanes DP, Thompson KG, and King DJ. Saccade target selection in frontal eye field of macaque. I. Visual and premovement activation. *J Neurosci* 15: 6905-6918, 1995a.

Schall JD, Morel A, King DJ, and Bullier J. Topography of visual cortex connections with frontal eye field in macaque: convergence and segregation of processing streams. *J Neurosci* 15: 4464-4487, 1995b.

Schall JD, Sato TR, Thompson KG, Vaughn AA, and Juan CH. Effects of search efficiency on surround suppression during visual selection in frontal eye field. *J Neurophysiol* 91: 2765-2769, 2004.

Schall JD, and Thompson KG. Neural selection and control of visually guided eye movements. *Annu Rev Neurosci* 22: 241-259, 1999.

Schiller PH, and Colby CL. The responses of single cells in the lateral geniculate nucleus of the rhesus monkey to color and luminance contrast. *Vision Res* 23: 1631-1641, 1983.

Schmolesky MT, Wang Y, Hanes DP, Thompson KG, Leutgeb S, Schall JD, and Leventhal AG. Signal timing across the macaque visual system. *J Neurophysiol* 79: 3272, 1998.

Softky WR, and Koch C. The highly irregular firing of cortical cells is inconsistent with temporal integration of random EPSPs. *J Neurosci* 13: 334-350, 1993.

Stanton GB, Goldberg ME, and Bruce CJ. Frontal eye field efferents in the macaque monkey: I. Subcortical pathways and topography of striatal and thalamic terminal fields. *J Comp Neurol* 271: 473-492, 1988.

Steinmetz NA, and Moore T. Changes in the response rate and response variability of area V4 neurons during the preparation of saccadic eye movements. *J Neurophysiol* 103: 1171-1178, 2010.

Thompson KG, and Bichot NP. A visual salience map in the primate frontal eye field. *Prog Brain Res* 147: 249-262, 2005.

Thompson KG, Bichot NP, and Schall JD. Dissociation of visual discrimination from saccade programming in macaque frontal eye field. *J Neurophysiol* 77: 1046-1050, 1997.

Thompson KG, Biscoe KL, and Sato TR. Neuronal basis of covert spatial attention in the frontal eye field. *J Neurosci* 25: 9479, 2005.

Thompson KG, Hanes DP, Bichot NP, and Schall JD. Perceptual and motor processing stages identified in the activity of macaque frontal eye field neurons during visual search. *J Neurophysiol* 76: 4040-4055, 1996.

Tolhurst DJ, Movshon JA, and Dean AF. The statistical reliability of signals in single neurons in cat and monkey visual cortex. *Vision Res* 23: 775-785, 1983.

Treisman AM, and Gelade G. A feature-integration theory of attention. *Cognitive Psychol* 12: 97-136, 1980.

Wang XJ. Synaptic basis of cortical persistent activity: the importance of NMDA receptors to working memory. *J Neurosci* 19: 9587-9603, 1999.

White BJ, and Munoz DP. Separate Visual Signals for Saccade Initiation during Target Selection in the Primate Superior Colliculus. *J Neurosci* 31: 1570, 2011.

Wichmann FA, and Hill NJ. The psychometric function: II. Bootstrap-based confidence intervals and sampling. *Perception & psychophysics* 63: 1314, 2001.

Wolfe JM. Guided Search 4.0: Current Progress with a model of visual search. In: *Integrated models of cognitive systems*, edited by W. G. New York: Oxford, 2007, p. 99-119.

Wolfe JM. What can 1 million trials tell us about visual search? *Psychol Sci* 9: 33-39, 1998.

Zhou H, and Desimone R. Feature-based attention in the frontal eye field and area V4 during visual search. *Neuron* 70: 1205-1217, 2011.

FIGURE CAPTIONS

Figure 1. Color and form visual search tasks. After fixating for a variable delay, a search array appeared consisting of a target and distractors. Monkeys were trained to make a single saccade to the location of the target for reward. **A**, Color search task with target-distractor similarity manipulation. Monkey F searched for a green or red target. Target-distractor similarity varied across trials. Target color varied across sessions. **B**, Form search task with set size manipulation. Monkeys Q and S searched for a rotated L among Ts or T among Ls. Set size varied across trials (2, 4, and 8 stimulus). Target identity was consistent within a session. Stimuli were arranged such that one distractor was always diametrically opposite the target location. **C**, Color search task with set size manipulation. Monkeys Q and S searched for a green or red target among red or green distractors, respectively. The task was otherwise identical to the form search task.

Figure 2. Temporal dynamics of discharge rate and Fano factor aligned on array onset for the full population of 304 neurons during all visual search tasks. **A**, Mean discharge rate (lines) and ±SE (shading) was computed in a 50 ms sliding window separately for trials in which the target or a distractor was in the RF. Gray dots indicate significance from baseline (100 ms before array onset) in steps of 10 ms when the target (dark gray) or distractors (light gray) were in the RF (Wilcoxon ranked-sum test, $p < 0.01$). Black dots indicate significant differences between discharge rates when the target or distractors were in the RF. The dotted vertical line indicates the selection time (ST),

which is the time when the distribution of discharge rates for trials in which the target versus distractor were in the RF first diverged significantly for 5 consecutive time bins. **B**, Mean Fano factor computed in same analysis windows as described above. There is no ST labeled because the distribution of Fano factors for trials in which the target versus distractor were in the RF never significantly diverged. The brief, but non-significant separation around ~190ms can be attributed to saccade initiation. **C**, Distribution of differences in discharge rate when the target or a distractor was in the neurons' RFs computed in the post-stimulus epoch 100 ms after array presentation until 100 ms before mean saccade response time. Asterisks denote significant difference from 0 (Wilcoxon signed-rank test, *** denotes $p < 0.001$). **D**, Distribution of differences for Fano factor.

Figure 3. Temporal dynamics of discharge rate (top) and Fano factor (bottom) for efficient (left) and inefficient (right) search. Conventions as in Figure 2.

Figure 4. Effect of luminance on discharge rate (DR) and Fano factor (FF). **A**, Mean discharge rate (±SE) divided by target luminance (Low: 0.01 to 0.6 cd/m^2; Medium: 0.20 to 1.00 cd/m^2; High: 1.70 to 5.00 cd/m^2). Gray dots indicate significant differences from baseline (Wilcoxon rank-sum test, $p < 0.01$). Inset shows mean-matched discharge rate for each luminance group (see Materials and Methods; Churchland et al., 2010). The mean-matched discharge rate is invariant across time and luminance. **B**, Variations in Fano factor with luminance. Conventions as in panel A. Fano factor decreases significantly with luminance even when controlling for changes in mean discharge rate.

C, Distribution of slopes of mean discharge rate as a function of luminance group in the post-stimulus epoch (sp/s/cd/m^2). Inset shows mean discharge rate (±SE) by luminance group. Asterisks denote significant difference of mean value from 0 (Wilcoxon signed-rank test, *** denotes $p < 0.001$). **D**, Same as panel C for Fano factor (Fano factor/cd/m^2). Note that discharge rate and Fano factor were computed using 150 ms time bins, therefore the visual latency may appear earlier due to temporal smearing. All latency estimates reported in the text used smaller 50 ms time bins.

Figure 5. Effect of set size on discharge rate (DR) and Fano factor (FF) for trials in which the target (left) or distractors (right) were in the neurons' RFs. Mean discharge rate (top, **A,B**) and Fano factor (bottom, **C,D**) aligned on array onset for set size 2 (gray), 4 (blue), and 8 (red). Insets show mean discharge rate or Fano factor (±SE) for each set size in the time interval 50-125 ms after array onset (shaded region). Black dots indicate times in which slope of the least squares regression line for discharge rate and Fano factor as a function of set size decreased significantly ($p < 0.01$). The regression line was computed by averaging discharge rate and Fano factor across time bins for each set size in a running window (±20 ms) incremented in time steps of 10ms.

Figure 6. Effect of set size on discharge rate (DR) and Fano factor (FF) during efficient (left) and inefficient (right) visual search. Population histogram for slope coefficient of least squares regression line fit to mean discharge rate (**A,C**, top) and Fano factor (**B,D**, bottom) in the early visual epoch 50-125 ms after array onset as a function of set size during efficient (left) and inefficient (right) search. Inset shows population mean (±SE)

discharge rate (DR) or Fano factor (FF) for each set size. Asterisks indicate that the population of slopes was significantly shifted from 0 (Wilcoxon signed-rank test, ** $p < 0.01$; *** $p < 0.001$).

Figure 7. Temporal dynamics of discharge rate (**A**) and Fano factor (**B**) aligned on saccade initiation during visual search for the full population of 304 neurons. Conventions as in Figure 2. **C**, Distribution of difference in discharge rate when the saccade was directed towards or away from the neuron's RF in the pre-saccade epoch (50-0 ms before saccade). Asterisks denote significance from 0 (Wilcoxon signed-rank test, *** denotes $p < 0.001$). **D**, Same as panel C, but for Fano factor.

Figure 8. Mean-matched discharge rate (DR) (top) and Fano factor (bottom) as a function of time relative to array presentation (left) and saccade initiation (right). Solid vertical line indicates time of saccade. Mean-matching was performed across target locations and saccade directions, but independently for array-aligned and saccade-aligned data. Conventions as in Figure 2.

Figure 9. Spatial tuning of mean discharge rate (**A,C**) and Fano factor (**B,D**) as a function of distance from RF center (in degrees polar angle) during the post-array (left) and pre-saccadic (right) epochs. Solid lines are best fitting Gaussian curves. Dashed line is the mean across locations for data that did not exhibit significant selectivity in the interval of interest. Error bars are SE.

Figure 10. Visually-responsive and saccade-related subpopulations. Mean discharge rate (**A,C**) and Fano factor (**C,D**) for visually-responsive (left) and saccade-related (right) neurons during visual search. Conventions as in Figure 2.

Figure 11. Accumulator model simulations. Simulated model discharge rates (DR) (top) and Fano factor (FF) (bottom) relative to array onset (left) and saccade (right). Lines are the averages (±SE) across 304 simulated neurons with 110 simulated trials to match the statistical power of the observed data. Gray histogram (top) is the quantile averaged response time (RT) probability distribution across all simulations. Only one accumulator representing a saccade to the neurons' response field was simulated. Note that Fano factor begins declining ~50 ms after target onset and reaches a minimum at the time of saccade initiation as observed in FEF neurons (see Figure 10C,D).

Figure 12. Memory-guided saccades. Mean discharge rate (**A**) and Fano factor (**B**) during memory-guided saccades aligned to target onset (left) or saccade (right) in which the target appeared inside (dark gray, Target in RF) or diametrically opposite (light gray, Target opp RF) the neurons' RFs. Stimulus duration was 80-150 ms and delay intervals ranged from 500-1000 ms. Insets show mean-matched discharge rate and Fano factor. Conventions as in Figure 2.

Figure 13. Mean discharge rate (**A,C**) and Fano factor (**B,D**) aligned on the cue (left) and saccade (right) for memory-guided saccade trials with RT earlier (green) and later

(red) than median RT. The thin colors lines in panel (**A,C**) indicate cumulative distributions of fast (green) and slow (red) RTs. This analysis includes all neurons recorded during the memory-guided saccade task and all trials regardless of whether the target was inside or opposite the neurons' RFs. Whereas discharge rate varied with RT mainly after the response cue, Fano factor varied with RT mainly before the response cue. Discharge rate and Fano factor were indistinguishable across RT samples at the time of saccade initiation.

Table 1. Values are mean difference ± SE. Asterisks denote significant differences (Wilcoxon sign-rank test; * for $p < 0.05$, ** for $p < 0.01$, *** for $p < 0.001$).

A. Color search: Target-distractor similarity

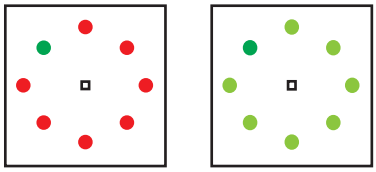

B. Form search: Set-size

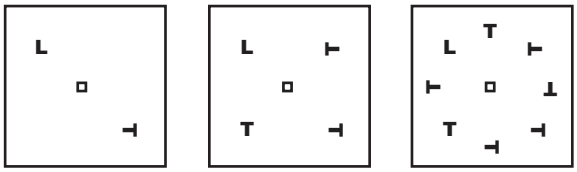

C. Color search: Set-size

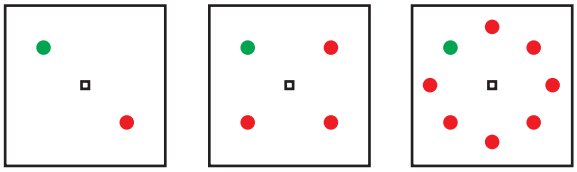

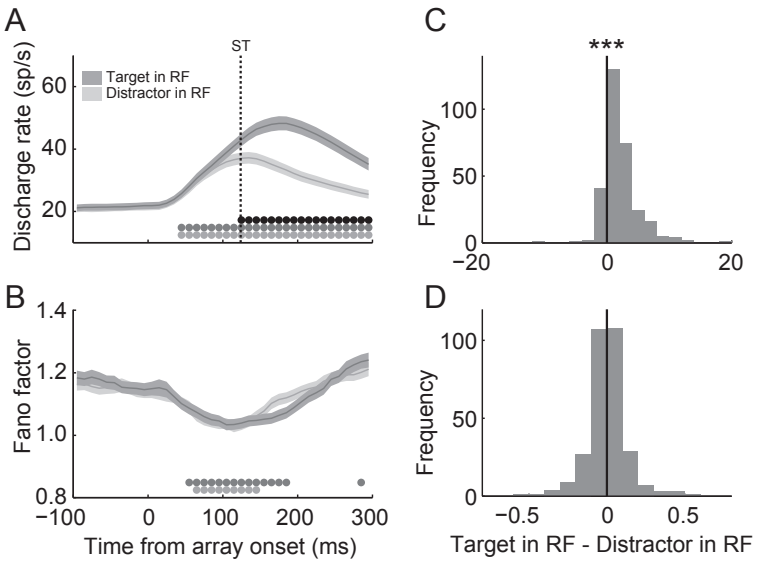
A
ST
Target in RF
Distractor in RF
Discharge rate (sp/s)
60
40
20
B
Fano factor
1.4
1.2
1.0
0.8
−100
0
100
200
300
Time from array onset (ms)
C
***
Frequency
100
50
0
−20
0
20
D
Frequency
100
50
0
−0.5
0
0.5
Target in RF - Distractor in RF

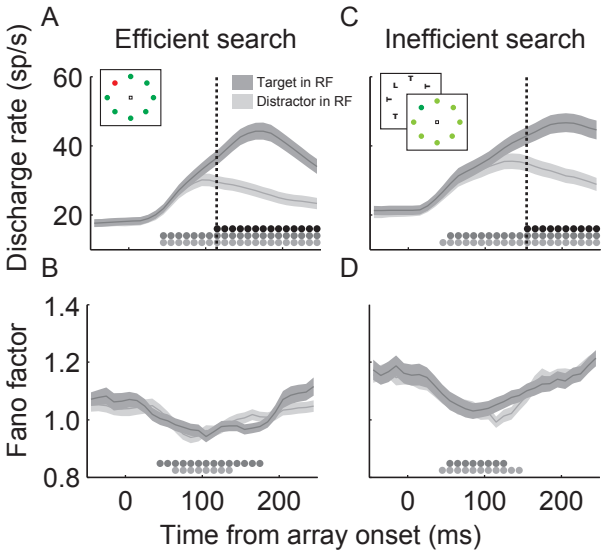
A
Efficient search
C
Inefficient search
Target in RF
Distractor in RF
Discharge rate (sp/s)
60
40
20
B
D
Fano factor
1.4
1.2
1.0
0.8
0
100
200
Time from array onset (ms)

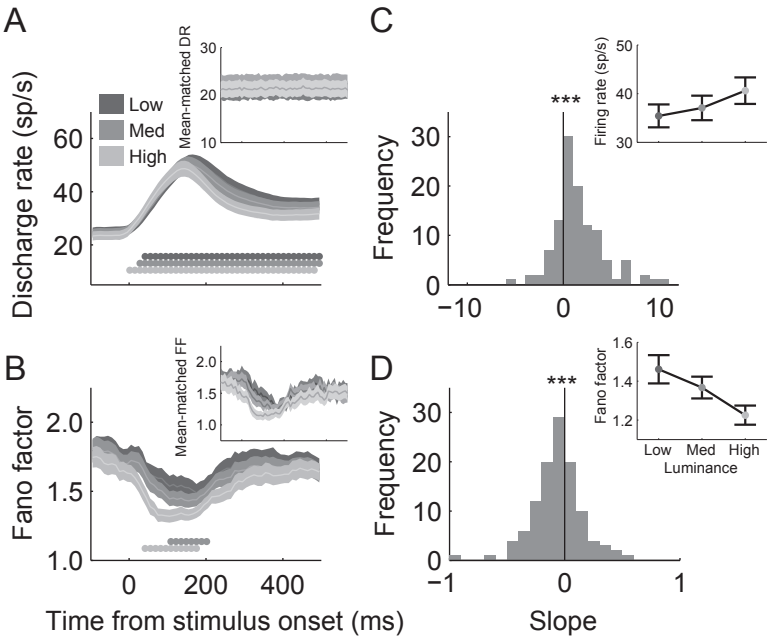
A
B
C
D
Discharge rate (sp/s)
Low
Med
High
Mean-matched DR
Fano factor
Mean-matched FF
Time from stimulus onset (ms)
Frequency
***
Firing rate (sp/s)
Fano factor
Low Med High
Luminance
Slope

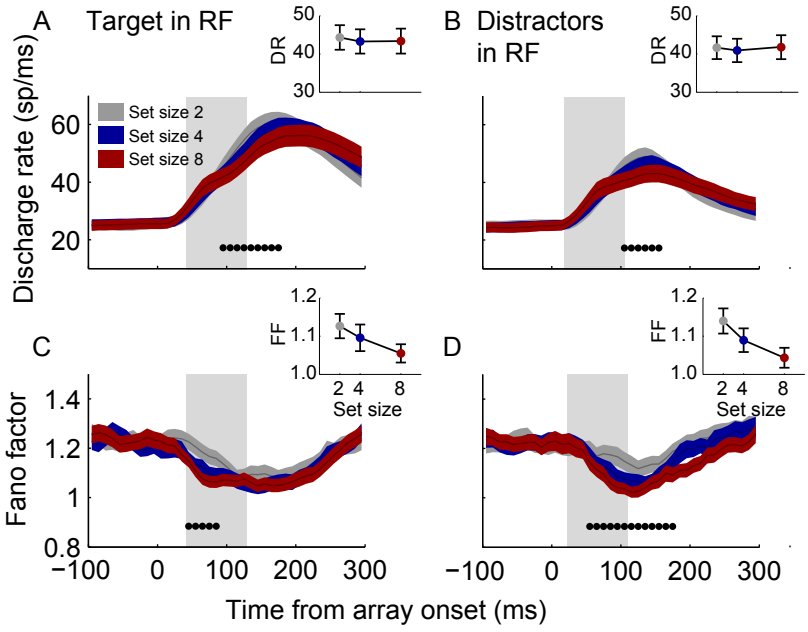
A
Target in RF
B
Distractors
in RF
C
D
Discharge rate (sp/ms)
Fano factor
Set size 2
Set size 4
Set size 8
DR
FF
Set size
Time from array onset (ms)

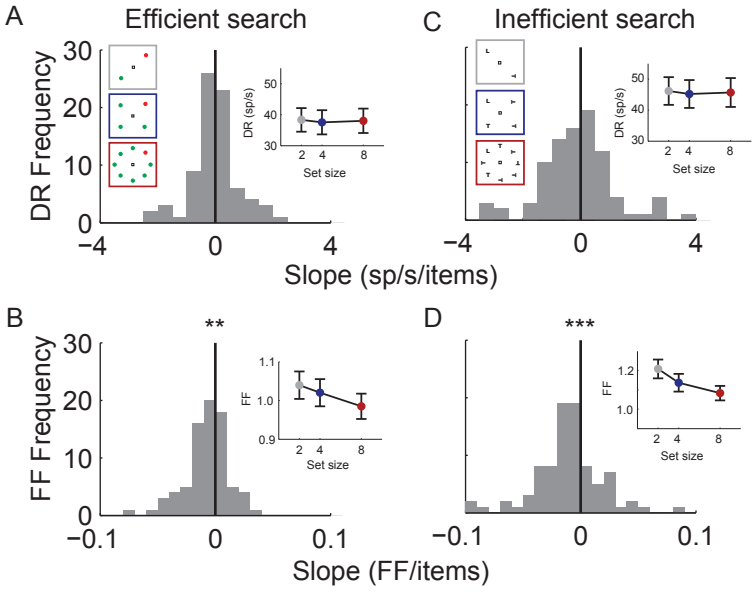
A
Efficient search
C
Inefficient search
DR Frequency
30
20
10
0
−4
0
4
DR (sp/s)
50
40
30
2 4 8
Set size
Slope (sp/s/items)
B
**
D
***
FF Frequency
FF
1.1
1.0
0.9
1.2
−0.1
0.1
Slope (FF/items)

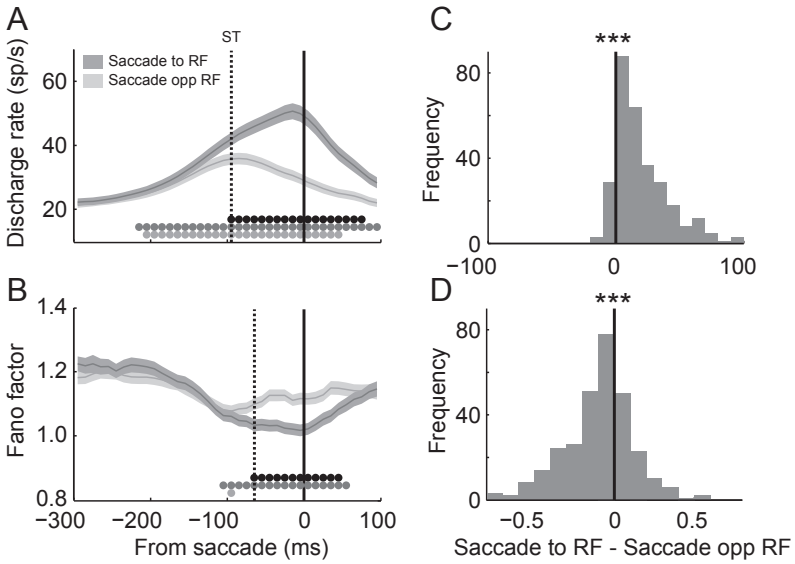
A
ST
Saccade to RF
Saccade opp RF
Discharge rate (sp/s)
60
40
20
B
Fano factor
1.4
1.2
1.0
0.8
−300
−200
−100
0
100
From saccade (ms)
C
***
Frequency
80
40
0
−100
0
100
D
***
Frequency
80
40
0
−0.5
0
0.5
Saccade to RF - Saccade opp RF

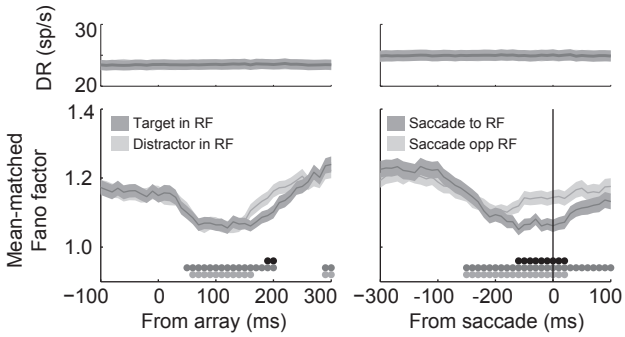
DR (sp/s)
30
20
Mean-matched Fano factor
1.4
1.2
1.0
Target in RF
Distractor in RF
Saccade to RF
Saccade opp RF
−100
0
100
200
300
From array (ms)
−300
-100
-200
0
100
From saccade (ms)

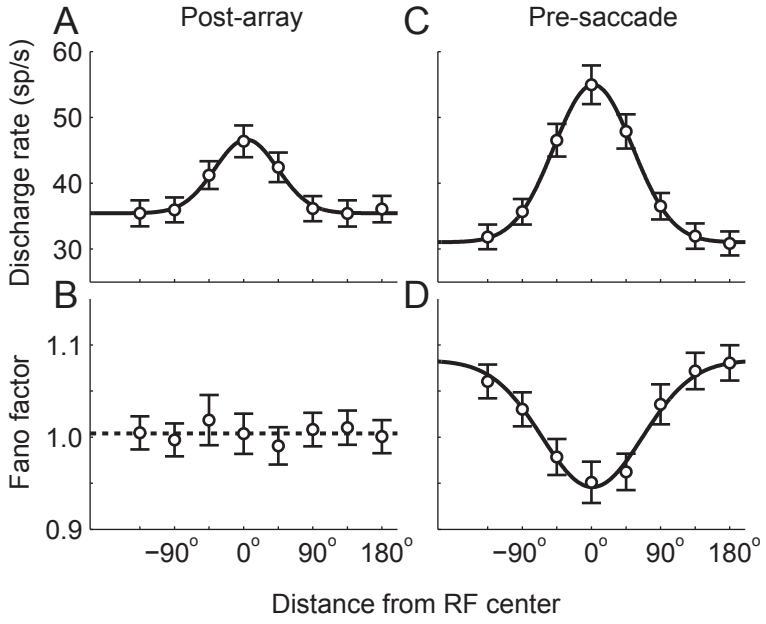
A
Post-array
C
Pre-saccade
Discharge rate (sp/s)
60
50
40
30
B
D
Fano factor
1.1
1.0
0.9
−90°
0°
90°
180°
Distance from RF center

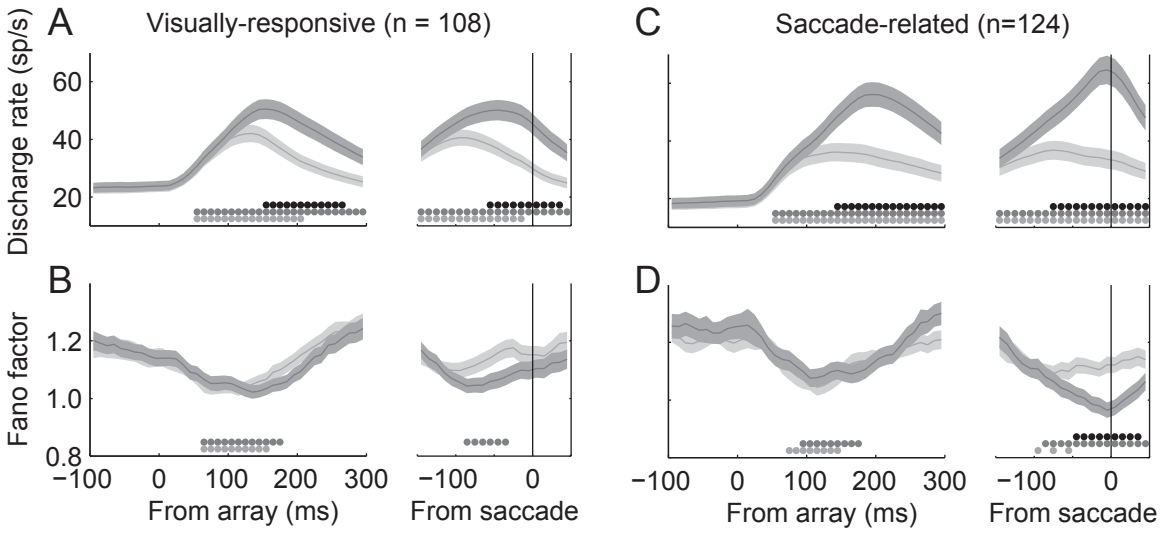
A
Visually-responsive (n = 108)
C
Saccade-related (n=124)
Discharge rate (sp/s)
60
40
20
B
D
Fano factor
1.2
1.0
0.8
−100
0
100
200
300
From array (ms)
−100
0
From saccade

Figure 11

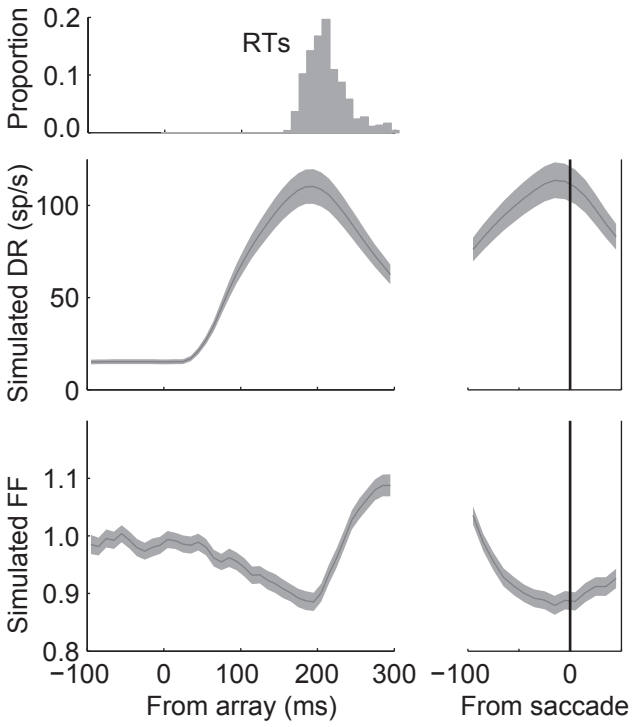
Proportion
0.2
0.1
0.0
RTs
Simulated DR (sp/s)
100
50
0
Simulated FF
1.1
1.0
0.9
0.8
−100
0
100
200
300
From array (ms)
−100
0
From saccade

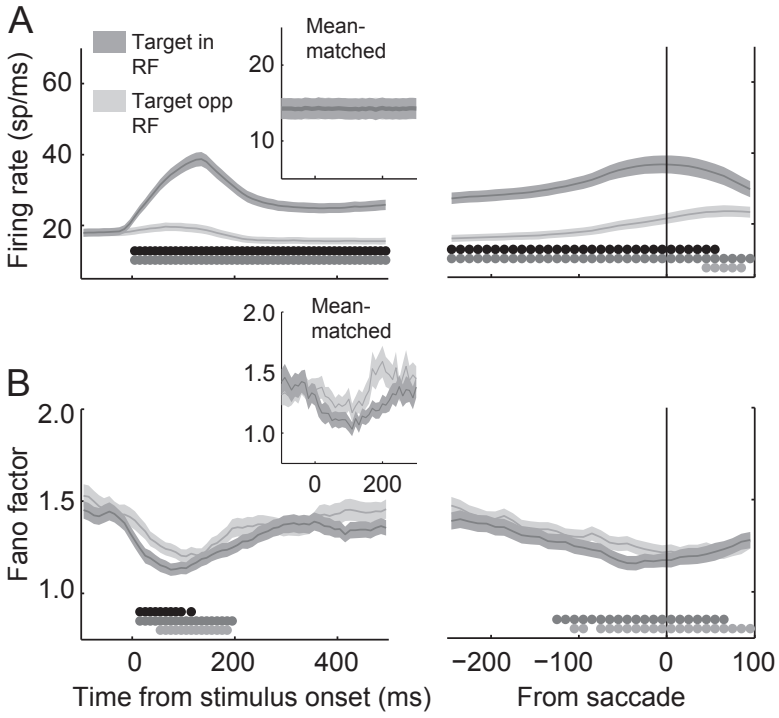
A
Target in RF
Target opp RF
Mean-matched
Firing rate (sp/ms)
60
40
20
20
10
B
Mean-matched
2.0
1.5
1.0
0
200
Fano factor
2.0
1.5
1.0
0
200
400
Time from stimulus onset (ms)
−200
−100
0
100
From saccade

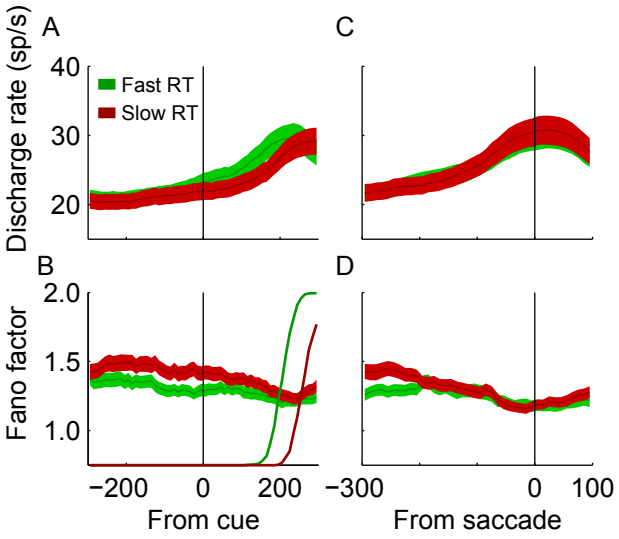
A
C
B
D
Discharge rate (sp/s)
40
30
20
Fast RT
Slow RT
Fano factor
2.0
1.5
1.0
−200
0
200
From cue
−300
0
100
From saccade

TABLE 1. Difference in mean discharge rate and Fano factor (±SE) for trials in which the target or distractors were in the RF.

	Post-array		Pre-saccade	
Color search				
	Monkey F		Monkey F	
Efficient				
Discharge rate	11.30 ± 2.82 ***		20.20 ± 4.48 ***	
Fano factor	0.01 ± 0.03		-0.06 ± 0.04	
Inefficient				
Discharge rate	3.40 ± 1.05 ***		19.04 ± 3.93 ***	
Fano factor	0.05 ± 0.03 *		-0.08 ± 0.04 *	
Inefficient form search				
	Monkey Q	Monkey S	Monkey Q	Monkey S
Set size 2				
Discharge rate	6.29 ± 0.98 ***	12.65 ± 2.97 ***	13.38 ± 2.00 ***	26.20 ± 4.46 ***
Fano factor	-0.01 ± 0.04	-0.01 ± 0.04	-0.07 ± 0.04 *	-0.11 ± 0.05 **
Set size 4				
Discharge rate	4.57 ± 0.89 ***	6.97 ± 2.02 ***	17.77 ± 2.56 ***	25.87 ± 4.11 ***
Fano factor	-0.05 ± 0.03	0.07 ± 0.10	-0.17 ± 0.04 ***	-0.05 ± 0.07 *
Set size 8				
Discharge rate	3.56 ± 0.65 ***	6.59 ± 2.29 **	19.13 ± 2.83 ***	27.02 ± 4.33 ***
Fano factor	0.01 ± 0.04	0.04 ± 0.05	-0.09 ± 0.04 **	-0.15 ± 0.04 **
Efficient color search				
Set size 2				
Discharge rate	4.22 ± 0.89 ***	4.41 ± 1.04 ***	7.73 ± 1.25 ***	11.82 ± 2.53 ***
Fano factor	-0.02 ± 0.03	0.02 ± 0.02	-0.04 ± 0.02 *	-0.07 ± 0.04
Set size 4				
Discharge rate	3.81 ± 0.63 ***	5.21 ± 0.82 ***	7.29 ± 1.28 ***	11.48 ± 2.42 ***
Fano factor	0.00 ± 0.02	-0.01 ± 0.03	-0.03 ± 0.02	-0.06 ± 0.03 *
Set size 8				
Discharge rate	4.34 ± 0.94 ***	3.93 ± 0.98 ***	8.92 ± 1.55 ***	12.04 ± 2.53 ***
Fano factor	-0.02 ± 0.02	0.04 ± 0.03	-0.02 ± 0.03	-0.03 ± 0.03